Diversity of photonic differentiators based on flexible demodulation of phase signals*

Zheng Ao-Ling(郑傲凌), Dong Jian-Ji(董建绩)†, Lei Lei(雷 蕾), Yang Ting(杨 婷), and Zhang Xin-Liang(张新亮)

Wuhan National Laboratory for Optoelectronics, School of Optoelectronic Science and Engineering, Huazhong University of Science and Technology, Wuhan 430074, *China*

(Received 16 June 2013; revised manuscript received 16 September 2013; published online 24 January 2014)

We theoretically propose a multifunctional photonic differentiation (DIFF) scheme based on phase demodulation using two cascaded linear filters. The photonic DIFF has a diversity of output forms, such as the 1st order intensity DIFF, the 1st order field DIFF and its inversion, and the 2nd-order field DIFF, depending on the relative shift between the optical carrier and the filter's resonant notches. As a proof, we also experimentally demonstrate the DIFF diversity using a phase modulator and two delay interferometers (DIs). The calculated average deviation is less than 7% for all DIFF waveforms. Our schemes show the advantages of flexible DIFF functions and forms, which may have different optical applications. For example, high order field differentiators can be used to generate complex temporal waveforms, and intensity differentiators are useful for the ultra-wideband pulse generation.

Keywords: photonic differentiator, pulse shaping, microwave photonics

PACS: 32.30.Bv, 84.40.–x, 42.79.Sz **DOI:** 10.1088/1674-1056/23/3/033201

1. Introduction

Photonic differentiation (DIFF) can offer a huge bandwidth of signal processing and immunity to electromagnetic interference compared to the traditional electronic DIFF. Thus photonic DIFF has been attracting lots of interest due to its potential wide applications in the ultrafast optical digital and analog processes.[1–5] The design and implementation of photonic DIFF is a primary step toward the practical optical computing circuits.

To date, photonic DIFF can mainly be divided into two categories, the optical field DIFF and the optical intensity DIFF.[6] In the intensity DIFF, the output optical intensity signal is the mathematical DIFF of the input optical intensity, which could be used in ultra-wideband (UWB) microwave communications[7–9] and signal encoding.[10] The intensity DIFF could be implemented by incoherent photonic processors,[11] highly nonlinear fibers,[7] and semiconductor optical amplifiers (SOAs).[8,12,13] On the other hand, in the field DIFF, the output optical field (complex signal, including both amplitude and phase) is the DIFF of the input field signals, which has potential applications in ultrashort pulse generation,[3,14] a family of high order DIFF waveform generation,[15–17] and pulse edge recognition.[18] To date, the field DIFFs have been implemented by fiber Bragg gratings,[19,20] long-period fiber gratings,[2] interferometers,[16,21] SOAs,[14] and silicon integrated waveguides.[15,16,22,23] It is noticed that most of the aforementioned schemes are not versatile and show a sole function. Flexible and versatile DIFF functions are desirable to meet multi-requirements in photonic signal processing. Previously, we demonstrated the field DIFF and the intensity DIFF simultaneously based on phase modulation and optical filtering.[24] However a high order field DIFF is impossible in that scheme.

In this paper, to include more DIFF functions, we theoretically deduce and experimentally prove the diversity of the photonic DIFF based on phase demodulation assisted by two delay interferometers (DIs). The photonic differentiator can output a diversity of DIFF waveforms, such as the 1st order intensity DIFF, the 1st order field DIFF and its inversion, the 2nd order field DIFF, depending on the relative shift between the optical carrier and the filter resonant notches. The output waveforms have more formations compared to those in Ref. [24]. Our scheme shows the advantages of the flexible DIFF functions. For example, the high order field differentiators can be used to generate complex temporal waveforms, and the intensity differentiators are useful for the UWB pulse generation.

2. Operation principle

The operation principle is shown in Fig. 1. A tunable laser source (TLS) emits a continuous wave (CW) with a central wavelength of λ_0. A phase modulator (PM) is driven by an electrical temporal signal $s(t)$ to modulate the

*Project supported by the National Basic Research Program of China (Grant No. 2011CB301704), the Program for New Century Excellent Talents in Universities of China (Grant No. NCET-11-0168), the Foundation for the Author of National Excellent Doctoral Dissertation of China (Grant No. 201139), and the National Natural Science Foundation of China (Grant Nos. 60901006 and 11174096).

†Corresponding author. E-mail: jjdong@mail.hust.edu.cn

© 2014 Chinese Physical Society and IOP Publishing Ltd

CW. Two cascaded DIs with their notch wavelengths of λ_{p1} and λ_{p2} follow the PM. The frequency response of the DI can be approximately regarded as a linear response near the notch frequency.[16] According to the theoretical analysis in Refs. [24] and [25], the output optical power of the first DI (DI_1) can be expressed as

$$P_{out1} = (\omega_0 - \omega_{p1})^2 + 2\beta(\omega_0 - \omega_{p1})\frac{\partial s(t)}{\partial t} + \left(\beta\frac{\partial s(t)}{\partial t}\right)^2, \quad (1)$$

where ω_0 and ω_{p1} are the optical carrier frequency and the notch angular frequency of DI_1, respectively, satisfying $\omega_i = 2\pi c/\lambda_i$, $i = 0$, p1, and β is the phase-modulated index.

Assume that the notch of the DI is aligned exactly to the optical carrier. Then Eq. (1) can be simplified approximately as

$$P_{out1} \approx \left(\beta\frac{\partial s(t)}{\partial t}\right)^2. \quad (2)$$

Output waveforms of this form can be defined as the 1st order field DIFF of the input signals, since the power of the outputs is proportional to the square of the differentiation of the input signals.[25]

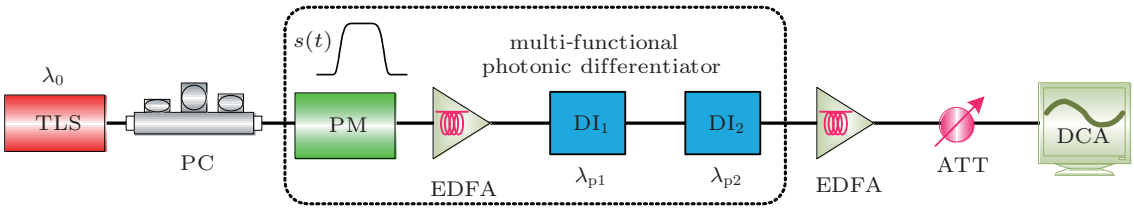


Fig. 1. (color online) Experimental setup for the proposed multifunctional differentiators (TLS: tunable laser source; ATT: attenuator; EDFA: erbium doped fiber amplifier; PM: phase modulator; DI: delay interferometer; DCA: digital communication analyzer; PC: polarization controller).

Assume that the notch of the DI is not aligned to the optical carrier, then the third term of Eq. (1) is far smaller than the other two terms. Then Eq. (1) can be simplified as

$$P_{out1} \approx (\omega_0 - \omega_{p1})^2 + 2\beta(\omega_0 - \omega_{p1})\frac{\partial s(t)}{\partial t}. \quad (3)$$

Output waveforms of this form can be defined as the 1st order intensity DIFF of the input signals, since the power of the outputs is proportional to the differentiation of the input signals.[25]

With a simple mathematical derivation, the output optical power of the second DI (DI_2) can be expressed as

$$P_{out2} = \left(\beta\frac{\partial s(t)}{\partial t} + \omega_0 - \omega_{p1}\right)^2\left(\beta\frac{\partial s(t)}{\partial t} + \omega_0 - \omega_{p2}\right)^2 + \left(\beta\frac{\partial^2 s(t)}{\partial t^2}\right)^2, \quad (4)$$

where ω_{p2} is the central frequency of DI_2, satisfying $\omega_{p2} = 2\pi c/\lambda_{p2}$.

If we define $\omega_1 = \omega_0 - \omega_{p1}$ and $\omega_2 = \omega_0 - \omega_{p2}$, then Eq. (4) can be simplified as

$$P_{out2} = \left[\left(\beta\frac{\partial s(t)}{\partial t}\right)^2 + \beta(\Delta\omega_1 + \Delta\omega_2)\frac{\partial s(t)}{\partial t} + \Delta\omega_1\Delta\omega_2\right]^2 + \left(\beta\frac{\partial^2 s(t)}{\partial t^2}\right)^2. \quad (5)$$

Equation (5) suggests that the output power contains lots of DIFF forms, such as the 1st order DIFF, the square of the 1st order DIFF and the 2nd order DIFF, and their product terms. Since Eq. (5) is a very complex equation, one may simplify it under certain specific conditions.

2.1. Case 1: the first-order intensity DIFF

Equation (5) can be simplified into four cases, which represent four different DIFF forms, respectively. In the first case, assume that the wavelength notches of both DIs are located at the same side of the wavelength of the optical carrier and misaligned to the notches. To simplify Eq. (5), there are several approximations used, 1) the phase modulation index β is very small, 2) the misalignment of ω_1 and ω_2 is very small so that the DI response meets the linear response, and 3) the output power of the high order DIFF term is much lower than that of the 1st order DIFF term. These approximations are easily satisfied in practical experiments. Then Eq. (5) can be simplified approximately as

$$P_{out2} \approx 2\beta\Delta\omega_1\Delta\omega_2(\Delta\omega_1 + \Delta\omega_2)\frac{\partial s(t)}{\partial t} + (\Delta\omega_1\Delta\omega_2)^2. \quad (6)$$

Equation (6) has the same form as Eq. (3), which suggests the 1st order intensity DIFF of the input signals. Figure 2 shows the output temporal waveforms of DI_1 and DI_2 when the input signal is a super-Gaussian pulse according to Eq. (5). The input super-Gaussian pulse is shown as S1 in Fig. 2, and the calculated output temporal waveforms of DI_1 and DI_2 are shown as S2 and S3 in Fig. 2. In the following, S1–S3 represent the same meanings as those in Fig. 2 without specific statements.

The pulse width of the input signal is set at 200 ps. In the simulation, we set $\lambda_{p1}-\lambda_0=\lambda_{p2}-\lambda_0=0.1$ nm in Fig. 2(a), and set $\lambda_{p1}-\lambda_0=\lambda_{p2}-\lambda_0=-0.1$ nm in Fig. 2(b). One can see that the output waveform of DI_2 is exactly the 1st order intensity DIFF result. At the same time, the DIFF waveforms of Figs. 2(a) and 2(b) are polarity reversed, which can be explained by Eq. (6). The polarity-reversed DIFF waveforms can be used in the pulse polarity modulation of UWB signals.

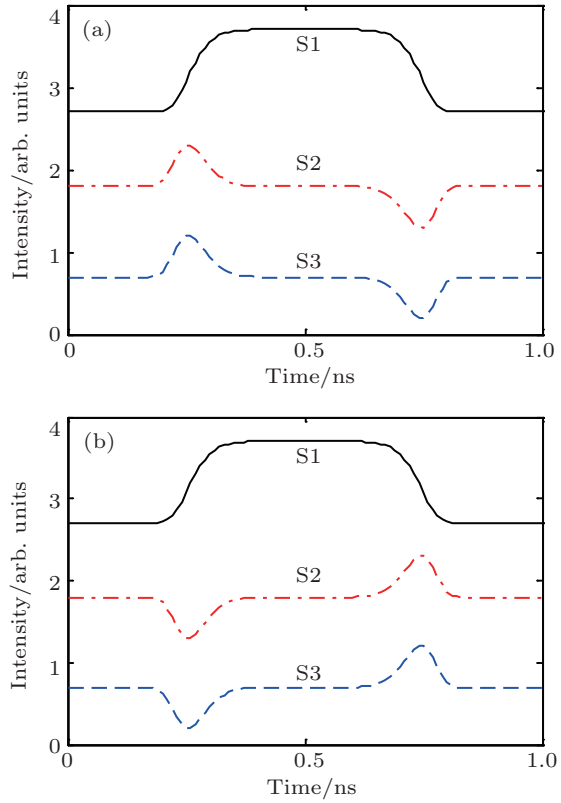


Fig. 2. (color online) Simulated waveforms for the 1st order intensity DIFF: (a) $\lambda_{p1}-\lambda_0=\lambda_{p2}-\lambda_0=0.1$ nm; (b) $\lambda_{p1}-\lambda_0=\lambda_{p2}-\lambda_0=0.1$ nm.

2.2. Case 2: the first-order field DIFF

In the second case, assume that the notch of one DI is exactly aligned to the optical carrier, whereas the notch of the other DI is misaligned. Under the same approximations as those in case 1, Eq. (5) can be simplified as

$$P_{out2}\approx[\beta(\Delta\omega_1+\Delta\omega_2)]^2\left(\frac{\partial s(t)}{\partial t}\right)^2. \tag{7}$$

Equations (2) and (7) have the same form, indicating that the output power is the 1st order field DIFF. Figure 3 shows the output temporal waveforms of DI_1 and DI_2 when the input signal is a super-Gaussian pulse based on Eq. (5). In the simulation, the pulse width of the input signal is still set at 200 ps, the wavelength misalignment of one DI is set at ±0.1 nm, and the other is set at zero, as shown in Figs. 3(a)–3(d), respectively. It is proved that all the output waveforms of DI_2 are the same, with the square of the first-order DIFF waveform. This field DIFF can be used to extract the pulse edges and suppress the signal noise with a direct current (DC) in optical signal processing systems.

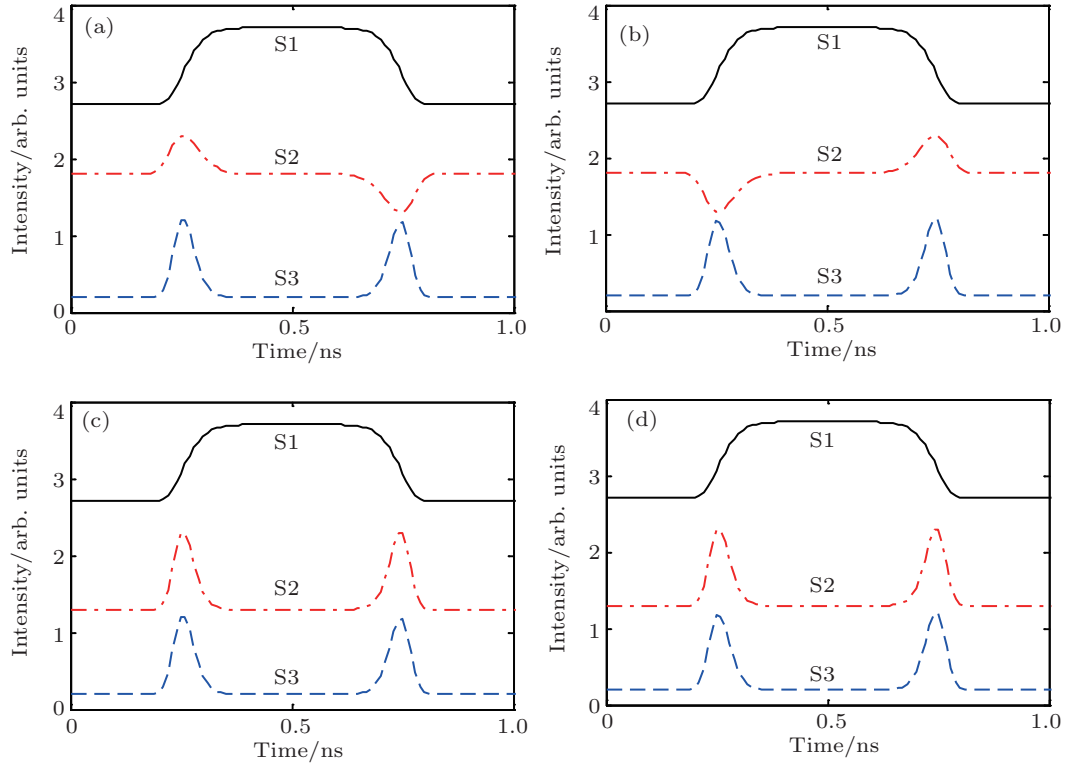


Fig. 3. (color online) Simulated waveforms for the 1st order field DIFF: (a) $\lambda_{p1}-\lambda_0=0.1$ nm, $\lambda_{p2}-\lambda_0=0$ nm, (b) $\lambda_{p1}-\lambda_0=-0.1$ nm, $\lambda_{p2}-\lambda_0=0$ nm, (c) $\lambda_{p1}-\lambda_0=0$ nm, $\lambda_{p2}-\lambda_0=0.1$ nm, (d) $\lambda_{p1}-\lambda_0=0$ nm, $\lambda_{p2}-\lambda_0=-0.1$ nm.

2.3. Case 3: the first-order field DIFF in inversion

In the third case, assume that the notches of the two DIs are both misaligned to the optical carrier, but symmetrically distributed on the opposite sides of the optical carrier. For example, we set $\lambda_{p1}-\lambda_0=0.1$ nm and $\lambda_{p2}-\lambda_0=-0.1$ nm. Then $\beta(\omega_1+\omega_2)\partial s(t)/\partial t=0$. With the approximation of a small phase modulation index, Eq. (5) can be simplified as

$$P_{\text{out2}}\approx 2\beta^2\Delta\omega_1\Delta\omega_2\left(\frac{\partial s(t)}{\partial t}\right)^2+(\Delta\omega_1\Delta\omega_2)^2. \tag{8}$$

Since $\Delta\omega_1\Delta\omega_2<0$, the first term of the right hand side (RHS) of Eq. (8) is opposite to the square of the optical field DIFF, and the second term is a positive constant. Therefore, the output waveform is a field DIFF with an inversion. Figure 4 shows the simulated output waveforms of DI_1 and DI_2, where $\lambda_{p1}-\lambda_0=0.1$ nm and $\lambda_{p2}-\lambda_0=-0.1$ nm in Fig. 4(a), and an opposite wavelength setting is used in Fig. 4(b). For injecting a super-Gaussian pulse, the output DIFF forms show two notches in the pulse edges of the input signals. This case demonstrates the totally inverted waveforms compared to case 2. So this type of DIFF may have similar applications to those of case 2.

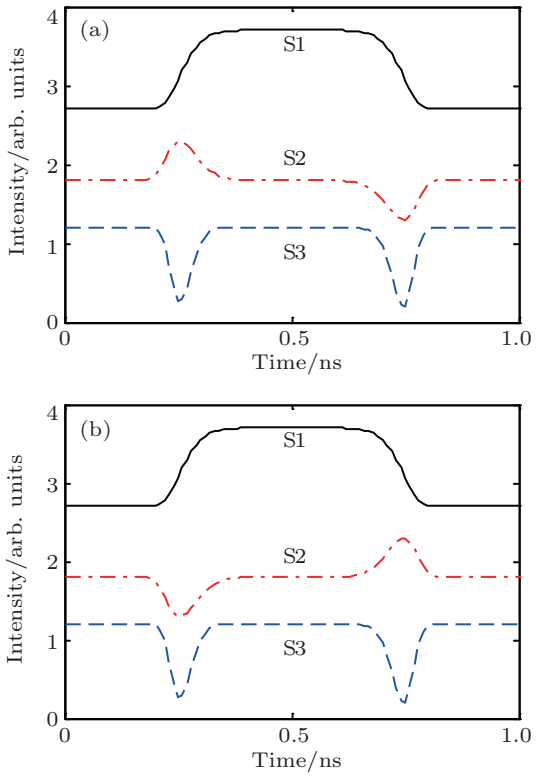


Fig. 4. (color online) Simulated waveforms for the 1st order field DIFF with an inversion: (a) $\lambda_{p1}-\lambda_0=0.1$ nm, $\lambda_{p2}-\lambda_0=-0.1$ nm, (b) $\lambda_{p1}-\lambda_0=-0.1$ nm, $\lambda_{p2}-\lambda_0=0.1$ nm.

2.4. Case 4: the second-order field DIFF

In the fourth case, assume that the notches of the two DIs are both aligned exactly to the optical carrier. That is to say, we set $\lambda_{p1}-\lambda_0=0$ nm and $\lambda_{p2}-\lambda_0=0$ nm. Thus $\Delta\omega_1=\Delta\omega_2=0$. Then Eq. (5) can be expressed as

$$P_{\text{out2}}=\left(\beta\frac{\partial s(t)}{\partial t}\right)^4+\left(\beta\frac{\partial^2 s(t)}{\partial t^2}\right)^2. \tag{9}$$

With the approximation of a small phase modulation index, the first term of the RHS of Eq. (9) can be ignored. Hence Eq. (9) can be further simplified as

$$P_{\text{out2}}\approx\left(\beta\frac{\partial^2 s(t)}{\partial t^2}\right)^2. \tag{10}$$

From Eq. (10), one can see that the output power is the square of the 2nd order field DIFF. Similar to the analysis of Eq. (2), the output power of this form can be defined as a second-order field DIFF. Figure 5 shows the simulated output waveforms of DI_1 and DI_2, where $\Delta\omega_1=\Delta\omega_2=0$. The output waveform of DI_2 accords well with the formation of the 2nd order field DIFF, although there is a little distortion. This distortion is caused by the term of the biquadrate of the 1st order DIFF, as indicated in Eq. (9). This kind of DIFF is a higher order DIFF, which may be useful to construct more complex temporal waveforms.

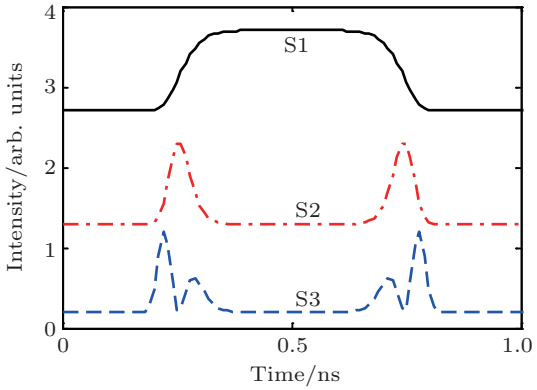


Fig. 5. (color online) Simulated waveforms for the 2nd order field DIFF, $\lambda_{p1}-\lambda_0=\lambda_{p2}-\lambda_0=0$.

From the aforementioned analysis and mathematical inference, we have demonstrated four kinds of DIFF formations, including the 1st order intensity DIFF, the 1st order field DIFF and its inversion, and the 2nd order field DIFF. These DIFF formations are dependent on the relative shift between the optical carrier and the DI resonant notches, which are summarized in Fig. 6. Therefore it is very easy to alter the DIFF formation by changing the laser wavelength or the DI resonant notches.

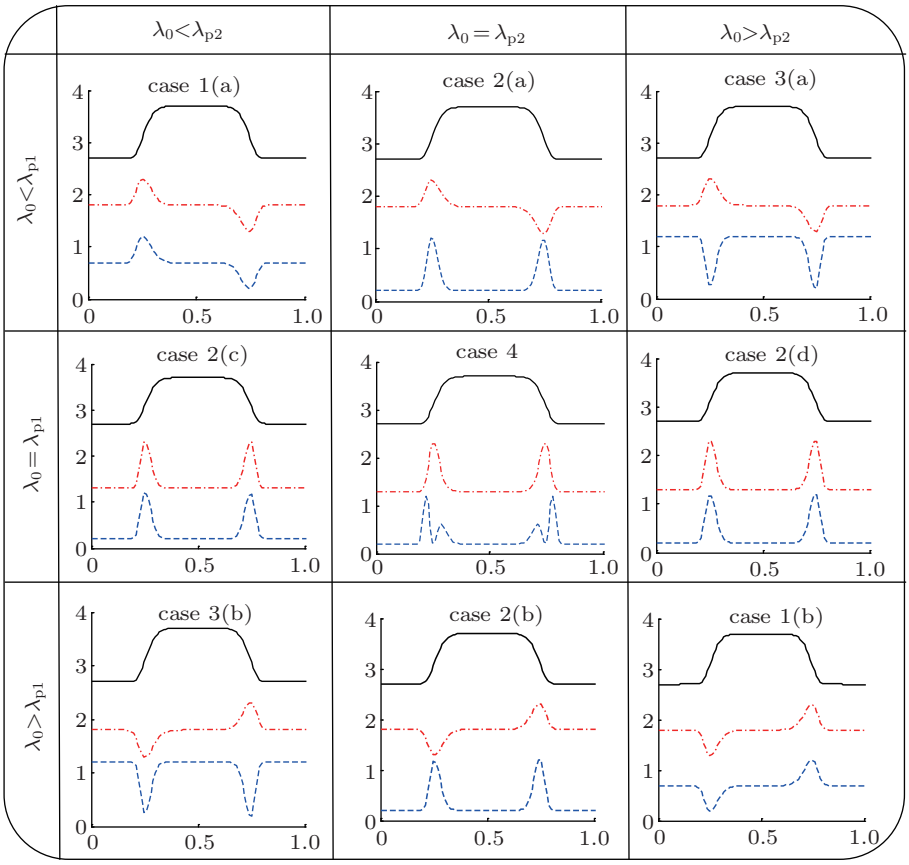


Fig. 6. (color online) Summary of all possible DIFF forms.

3. Experimental demonstration and discussion

In order to verify the feasibility of our scheme, a proof-of-concept experiment is carried out, as shown in Fig. 1. A CW beam is emitted from the TLS with a precisely tuning resolution of 1 pm. Then the CW beam is modulated by the PM. A polarization controller (PC) is placed before the PM to optimize the incident polarization state since the PM is polarization dependent. The PM (bandwidth: 40 GHz) is driven by an electrical super-Gaussian signal $s(t)$, which is generated by the bit pattern generator (BPG, SHF BPG 44E). The first erbium doped fiber amplifier (EDFA) is used to boost the input optical power. Two cascaded DIs have free spectral ranges (FSR) of 40 GHz and 100 GHz, respectively. The resonant frequencies of the DIs can be adjusted by the driving voltage. The output power is then optimized by the second EDFA and an attenuator (ATT), and measured by a digital communication analyzer (Agilent DCA86100C). The operation bandwidth of our scheme depends on the bandwidth of the PM, which is 40 GHz.

First the laser wavelength is set at 1563.9 nm and its output optical power is 13 dBm. The PM is driven by an electrical super-Gaussian pulse train with a repetition rate of 1.25 GHz, and the pulse width is about 200 ps, as shown in R1 of Fig. 7(a). Since the optical field could not be measured practically, all the DIFF results are analyzed with the optical power. In order to verify case 1, we set $\lambda_{p1} - \lambda_0 = \lambda_{p2} - \lambda_0 = 0.1$ nm. Then the output temporal waveforms of DI_1 and DI_2 are measured and shown as R2 and R3 in Fig. 7(a). The calculated waveforms are shown as S2 and S3, respectively, for comparison. One should notice that waveform R1 is the input waveform of both the measured outputs R2, R3 and the calculated outputs S2, S3 in Figs. 7 and 8. In the following, R1–R3 represent the same meanings as those in Fig. 7(a) without specific statements. One can see that the measured results have good agreements with the simulated ones. This experimental result can prove the case of the 1st order intensity DIFF, corresponding to the simulations of Fig. 2(a). In the following experiment, all parameters are maintained except the resonant notches of the DIs. In order to verify the 1st order field DIFF of case 2, we readjust the driving voltages of the DIs so that one DI notch is aligned and the other is misaligned to the laser wavelength. For this case, the measured output DIFF waveforms are shown in Fig. 7(b). One can see that the measured results have good agreements with the simulated ones. This experiment shows the 1st order field DIFF, corresponding to the simulations of Fig. 3(c).

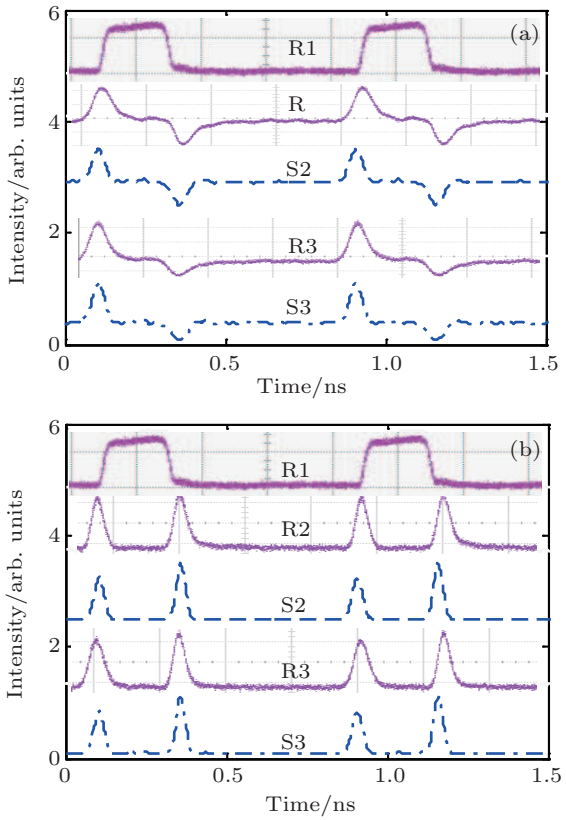


Fig. 7. (color online) Experimental results to show (a) case 1 and (b) case 2.

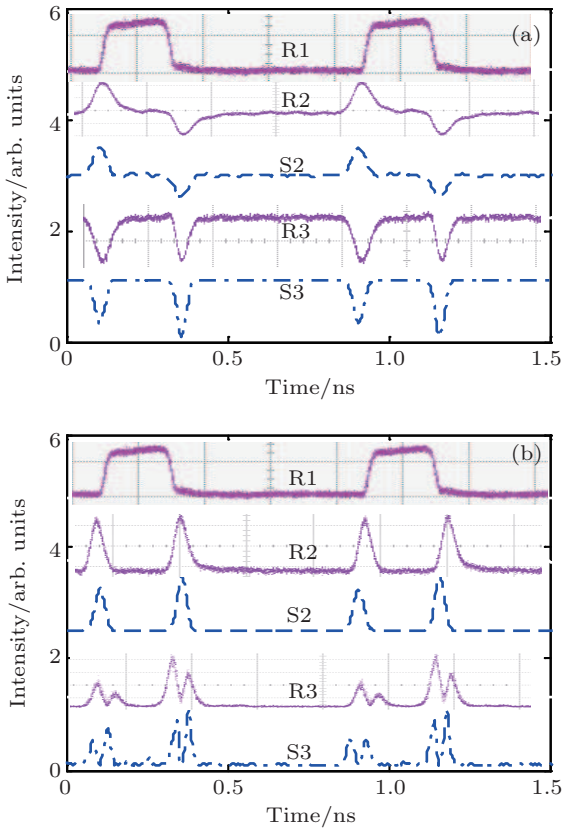


Fig. 8. (color online) Experimental results to show (a) case 3 and (b) case 4.

To verify case 3, the notches of the DIs are readjusted so that they are symmetrically distributed on the opposite sides of the laser wavelength, and the output DIFF waveforms are measured as shown in Fig. 8(a). One can see that the measured results have good agreements with the simulated ones. This experiment shows the 1st order field DIFF of inversion, corresponding to Fig. 4(a). Finally, the resonant notches of the DIs are adjusted so that they are exactly aligned to the laser wavelength. Figure 9 shows the transmission spectra of DI_1 and DI_2, the input laser wavelength, and the output spectrum of DI_2. DI_1 has an FSR of 40 GHz, and DI_2 has an FSR of 100 GHz. One can see that their resonant notches are aligned to the laser wavelength, i.e., 1563.9 nm. For this case, the output temporal waveforms of DI_1 and DI_2 are measured, as shown in Fig. 8(b). One can see that the measured results accord with the simulated ones except for a distortion. This distortion can be explained by Eq. (9). The experiment shows the 2nd order field DIFF, corresponding to the simulations of Fig. 5.

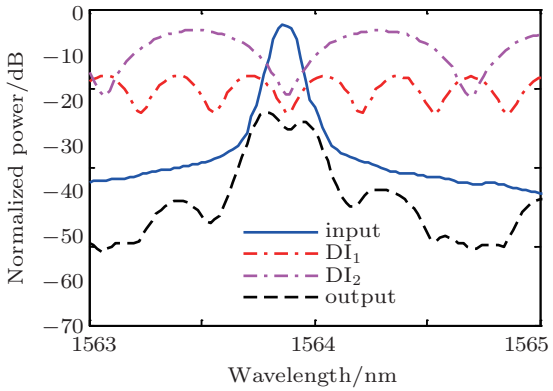


Fig. 9. (color online) Input and output spectra of the 2nd order field DIFF.

To analyze the DIFF accuracy, an average deviation is defined as the mean absolute deviation of the measured DIFF power from the calculated one on a certain pulse period,[15,16] which is set at 1500 ps in our experiment. Then the calculated average deviations for the 1st order intensity DIFF, the 1st order field DIFF, the reversed 1st order field DIFF, and the 2nd order field DIFF are 4.27%, 6.28%, 5.76%, and 6.28%, respectively. Table 1 shows all average deviations of the output waveforms of DI_1 and DI_2.

Table 1. Average deviations of all four DIFF results.

	Case 1	Case 2	Case 3	Case 4
DI_1 output	4.36%	6.78%	5.01%	6.59%
DI_2 output	4.27%	6.28%	5.76%	6.28%

4. Conclusion

We theoretically prove the diversity of the photonic DIFF based on phase demodulation using two cascaded linear filters. From mathematical inference and analysis, the photonic DIFF

can output four DIFF formations, including the 1st order intensity DIFF, the 1st order field DIFF, the reversed 1st order field DIFF, and the 2nd order field DIFF, depending on the relative shift between the optical carrier and the filter resonant notches. We also experimentally demonstrate the DIFF diversity using a phase modulator and two DIs. The total average deviations are less than 7% for all DIFF waveforms. Our schemes show the advantages of the flexible DIFF functions, which may have different optical applications.

References

[1] Azana J 2010 *IEEE Photonics Journal* **2** 359
[2] Slavik R, Park Y, Kulishov M, Morandotti R and Azana J 2006 *Opt. Express* **14** 10699
[3] Ngo N Q, Yu S F, Tjin S C and Kam C H 2004 *Opt. Commun.* **230** 115
[4] Slavik R, Park Y, Kulishov M and Azana J 2009 *Opt. Lett.* **34** 3116
[5] Li M, Shao L Y, Albert J and Yao J 2011 *IEEE Photonics Technology Letters* **23** 251
[6] Slavik R, Park Y, Krcmar D and Azana J 2009 *Opt. Commun.* **282** 2339
[7] Velanas P, Bogris A, Argyris A and Syvridis D 2008 *J. Lightw. Tech.* **26** 3269
[8] Dong J, Zhang X, Xu J, Shum P and Huang D 2007 *Opt. Lett.* **32** 1223
[9] Yao J 2009 *IEEE Microwav. Mag.* **10** 82
[10] Dong J, Yu Y, Zhang Y, Li X, Huang D and Zhang X 2011 *Opt. Express* **19** 10587
[11] Yongwoo P, Asghari M H, Helsten R and Azana J 2010 *IEEE Photonics Journal* **2** 1040
[12] Xu J, Zhang X, Dong J and Huang D 2007 *Opt. Lett.* **32** 3029
[13] Luo B, Dong J, Yu Y, Yang T and Zhang X 2013 *Chin. Phys. B* **22** 023201
[14] Li Z and Wu C 2009 *Opt. Lett.* **34** 830
[15] Dong J, Zheng A, Gao D, Liao S, Lei L, Huang D and Zhang X 2013 *Opt. Lett.* **38** 628
[16] Dong J, Zheng A, Gao D, Lei L, Huang D and Zhang X 2013 *Opt. Express* **21** 7014
[17] Dong J, Yu Y, Zhang Y, Luo B, Yang T and Zhang X 2011 *Photonics Journal* **3** 996
[18] Dong J, Zhang X, Fu S, Xu J, Shum P and Huang D 2008 *J. Sel. Top. Quantum Electron.* **14** 770
[19] Rivas L M, Singh K, Carballar A and Azana J 2007 *IEEE Photonics Technology Letters* **19** 1209
[20] Li M, Janner D, Yao J and Pruneri V 2009 *Opt. Express* **17** 19798
[21] Park Y, Azana J and Slavik R 2007 *Opt. Lett.* **32** 710
[22] Liu F, Wang T, Qiang L, Ye T, Zhang Z, Qiu M and Su Y 2008 *Opt. Express* **16** 15880
[23] Hu Y, Zhang L, Xiao X, Li Z, Li Y, Chu T, Su Y, Yu Y and Yu J 2012 *Journal of Optics* **14** 065501
[24] Dong J, Luo B, Zhang Y, Huang D and Zhang X 2011 *Opt. Commun.* **284** 5792
[25] Luo B, Dong J, Wang X, Huang D and Zhang X 2012 *Acta Phys. Sin* **61** 94213 (in Chinese)